40 лет ИТМ НАН Беларуси

M. H. HONG, POSCO DEPARTMENT KOREA, K. Y. CHOI, E. I. MARUKOVICH,
Y. A. LEBEDINSKY, A. M. BRANOVITSKY, Institute OF Metals Technology

УДК 621.74

ANALYSIS OF PRECIPITATION KINETICS OF MANGANESE AND COPPER SULFIDES IN INTERSTITIAL FREE STEELS

Introduction

In recent paper [1] the model of precipitation kinetic of copper and manganese sulfides was developed. Model is based on linear approximation of Gibbs energy change Δg during precipitation of copper sulfides:

$$\Delta g = Q \frac{\Delta T}{T_e} \frac{1}{V_m}, \tag{1}$$

where Q is proportional of enthalpy of phase transition and estimated by experimental data [2], and equilibrium temperature T_e estimated by thermodynamic calculations [3], V_m is molar volume.

Model of precipitation is based on classical theory of nucleation and growth and is presented in [1] with description of numeric methods for modeling. Now we present numerical calculations of precipitation kinetics. In the beginning we repeat basic formulas of this model.

According to classical nucleation theory, nucleation rate is given by

$$J^* = N_{tot} \beta^* Z \exp\left(-\frac{\Delta G^*}{kT}\right) \exp\left(-\frac{t_{inc}}{t}\right), \tag{2}$$

where N_{tot} – overall number of potential nucleation sites; β^* – frequency factor; Z – Zeldovich factor; ΔG^* – activation energy barrier and t_{inc} – incubation time:

$$\Delta G^* = \frac{4\pi}{3} R^{*2} \sigma = \frac{16\pi\sigma^3}{3\Delta g^2}, \tag{3}$$

σ is specific interfacial energy; R^* – critical radius,

$$R^* = \frac{R_0}{S}, \tag{4}$$

$$R_0 = \frac{2\sigma v_A}{kT}, \tag{5}$$

v_a – volume of precipitation molecule (Cu_2S stoichimetric composition assumed); T – temperature, $S = \ln\left(\frac{c_{Cu}^2 c_S}{c_{Cu2S}}\right)$, c_{Cu}, c_S – concentrations of solutes and c_{Cu2S} is product of solubility for equilibrium concentrations.
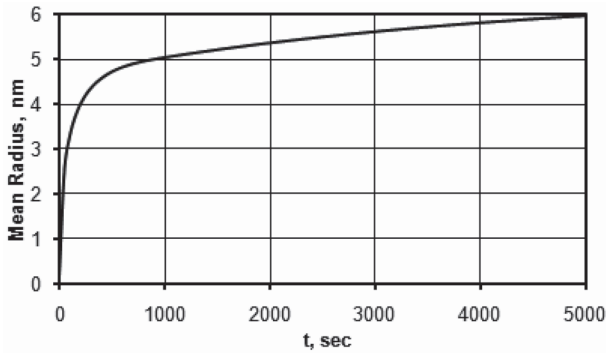
Fig. 1. Time evolution of average radius from the beginning of annealing

Homogeneous and heterogeneous nucleation and growth are modeling. For heterogeneous nucleation on dislocations the redefined values of activation barrier and mobility of atoms are considered.

Calculations

Independent copper sulfide precipitation

Initial concentrations of solutes is 0,07wt% for Cu and 0,04wt% for S. The values of relative nucleation rate J^*/N_{tot} for homogeneous nucleation and for heterogeneous nucleation are presented in Table 1. The maximum relative rate is approximately at 650 °C. It is very high nucleation rate value owing to high Cu diffusion on dislocations and small interface energy despite a small chemical free Gibbs energy of phase transition. Appreciable heterogeneous nucleation rate is observed even at low temperatures 200–300 °C.

In this modeling it is assumed, that nucleation and growth of Cu$_2$S precipitates occur at 650 °C during annealing process. Sites for heterogeneous nucleation are formed prior to annealing during hot and cold rolling processes. The nucleation density is assumed to be 10^{21} nuclei m^{-3}. This density is assumed for dislocation density of 10^{14} m^{-2} and distance of 100 nm between possible sites on linear dislocation [14].

The nucleation density for homogeneous nucleation is considerably higher, $N_{tot} \approx 2/a^3 \approx 10^{29}$, where a -lattice parameter of ferrite. In this section it is assumed, that actually these particles would be quickly dissolved due to the presence of more sizable Cu$_2$S inclusions with heterogeneous nucleation that have higher growth speed until its radius is less than R_{max}. Therefore, Cu$_2$S precipitation will be modeled only for heterogeneous nucleation. Heterogeneous nucleation is often regarded as the main mechanism of Cu$_2$S precipitation. The problem concerning simultaneous homogeneous and heterogeneous nucleation for

copper sulfide precipitation will be considered later. Now in this section the difference between activation energy for homo and heterogeneous nucleation will be also neglected due to huge instantaneous nucleation in any case.

The evolution of average precipitate radius is shown in Fig. 1. When the radius reaches the value of about 4–5 nm, the growth process is appreciably retarded. In this case the average inclusion radius of about 7 nm corresponds to practically complete depletion of Cu excess solutes in matrix. All concentrations mentioned here and below are molar. The ratio of current number of inclusions and the total number of possible sites for heterogeneous nucleation is practically equal to 1 after a few seconds of precipitation. In the absence of sulfur reactions with manganese or iron, inclusions of Cu$_2$S can monotonously grow in size that depends on initial solute concentrations.

It is known, that the particle size distribution function (PSD) calculated by this method often differs from experimental data. But qualitative analysis of PSD width is relevant and presented in this work. So, width of distribution function is narrow owing to actually simultaneous quick nuclei formation at the annealing onset.

Manganese sulfide precipitation

Solute concentrations of S 0,04 wt%, Mn 0,54 wt % in iron matrix. For approximation of Mn and S diffusion coefficients, interface energies and solubility products in γ - and α -Fe are used from the data [2].

Nucleation rate of MnS precipitation has satisfactorily high values for temperatures below 1200 °C (see table 2), so the modeling has been started from this temperature. It is assumed that after hot rolling at temperature near 900 °C the number of sites created is sufficient for occurring the heterogeneous nucleation.

Very low values less than 1 are not presented. The α − γ transition temperature is 911 °C and the total density of nucleation sites for homogeneous nucleation is 10^{29} m^{-3}, for heterogeneous nucleation 10^{20} m^{-3}.

For analysis of metastable behavior of copper sulfide precipitation relative to manganese sulfide, the annealing temperature in this and next sections is 700 °C. As earlier, the total density of nucleation sites for homogeneous nucleation is $2/a^3 \approx 10^{29}$ m^{-3}. It is assumed that heterogeneous nucleation takes place during and subsequent to hot rolling and the total initial density of possible sites is 10^{20} nuclei·m^{-3} for it. On annealing that follows cold rolling the total initial

T a b l e 1. **Relative nucleation rate for initial concentrations of Cu 0,07 wt% and S 0,04 wt%, s^{-1}**

Temperature, °C	200	250	300	350	400	450	500	550	600	650	700
Homogeneous	$1,62\cdot10^{-15}$	$8,35\cdot10^{-13}$	$1,42\cdot10^{-10}$	$1,04\cdot10^{-8}$	$3,97\cdot10^{-7}$	$8,86\cdot10^{-6}$	$1,26\cdot10^{-4}$	$1,21\cdot10^{-3}$	$7,66\cdot10^{-3}$	$2,57\cdot10^{-2}$	$1,03\cdot10^{-2}$
Heterogeneous	$6,21\cdot10^{-13}$	$1,80\cdot10^{-10}$	$1,92\cdot10^{-8}$	$9,52\cdot10^{-7}$	$2,59\cdot10^{-5}$	$4,33\cdot10^{-4}$	$4,81\cdot10^{-3}$	$3,70\cdot10^{-2}$	0,192	0,542	0,186

T a b l e 2. **Nucleation rates for initial concentrations of Mn – 0,54 wt% and S – 0,04 wt%, nuclei /s m^3**

Temperature °C	200	250	300	350	400	450	500	550	600	650
Homogeneous										
Heterogeneous	57,4	$1,32 \cdot 10^4$	$1,01 \cdot 10^6$	$3,20 \cdot 10^7$	$5,05 \cdot 10^8$	$4,41 \cdot 10^9$	$2,31 \cdot 10^{10}$	$7,67 \cdot 10^{10}$	$1,64 \cdot 10^{11}$	$2,32 \cdot 10^{11}$

Temperature °C	700	750	800	850	900	950	1000	1050	1100	1150
Homogeneous						$5,33 \cdot 10^{10}$	$1,44 \cdot 10^9$	$1,21 \cdot 10^7$	$2,16 \cdot 10^4$	4,85
Heterogeneous	$2,12 \cdot 10^{11}$	$1,21 \cdot 10^{11}$	$4,16 \cdot 10^{10}$	$7,77 \cdot 10^9$	$6,97 \cdot 10^8$	$6,10 \cdot 10^{15}$	$3,01 \cdot 10^{15}$	$9,56 \cdot 10^{14}$	$1,72 \cdot 10^{14}$	$1,47 \cdot 10^{13}$

density is higher, but nucleation of MnS in α – iron is very small. As is seen from Table 2, nucleation really occurs in γ-Fe at the temperatures close to α-Fe transition. Thus, nuclei of MnS are created during iron cooling before γ to α transformation. Therefore, time of such cooling plays an important role in MnS precipitation.

For the first calculation the dependence of temperature on time is approximated as cooling from 1200 °C at speed of 10 degree/sec until the annealing temperature of 700 °C is reached. Then isothermal annealing takes place.

The nucleation realized in this case is very small and the density of particles $\approx 10^{11}$ m^{-3}. The number of such particles is insufficient for notable changing of initial concentrations of solutes and effective sulfur removal from matrix.

For the second calculation it has been assumed that intermediate time delay is 300 seconds during hot rolling at temperature of 936 °C as compared with the first calculation (assuming $\alpha - \gamma$ temperature as 911 °C). Homo and heterogeneous nucleation have been modeled. The density for heterogeneous nucleation «jumps» from 0 to 10^{20} m^{-3} at the beginning of delay.

Fig. 2 illustrates the evolution of average radius. The average radius in conditions of sufficient number of solute excess in matrix is slightly dependent on nucleation rate and practically identical for both calculations. The evolution of solute concentrations in matrix is shown in Fig. 3. In this case the density of MnS inclusions is sufficient for appreciable sulfur removal even after 2000 seconds of annealing.

Simultaneous precipitation

Solute concentrations of Cu equal to 0,07 wt%, S 0,04 wt%, Mn 0.54 wt% in iron matrix. More complex results can be obtained for simulation of simultaneous homogeneous and heterogeneous precipitation of MnS and Cu$_2$S. In this case the concentration of only Cu is insufficient for precipitation of all sulfur. Mn concentration is much greater than corresponding sulfur concentration; because MnS precipitation has small nucleation rate and low nucleation density due to high interface energy of MnS creating. Therefore,

for effective interaction of Mn with S, the high manganese concentration and sufficiently long time of annealing for MnS growth are required. In the presence of satisfactory manganese concentration the interaction between sulfur and iron is neglected.

The temperature regime is identical to that in section 1,2 for MnS modeling including onset at 1200 °C, cooling at the speed of 10 °C/sec up to 936 °C, isothermal holding during 300 sec (with density for heterogeneous nucleation being 10^{20} nuclei·m^{-3} i. e. hot rolling simulation), cooling at the same speed until reaching the annealing temperature and isothermal annealing at 700 °C. In this time interval the density for heterogeneous nucleation is increased to·10^{21} nuclei/m^3 after cold rolling. Cooling to cold rolling temperature and subsequent heating to annealing temperature were neglected.
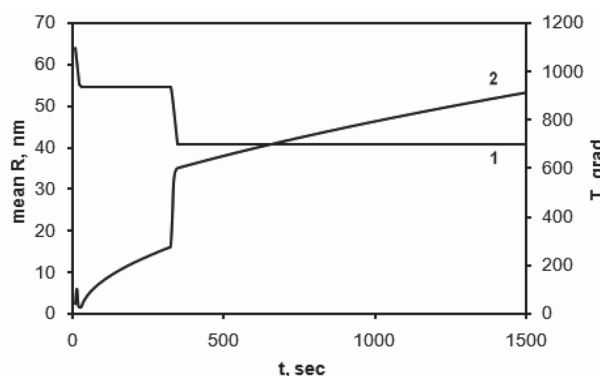

Fig. 2. Temperature (*1*) and average radius (*2*) of MnS inclusion depending on time
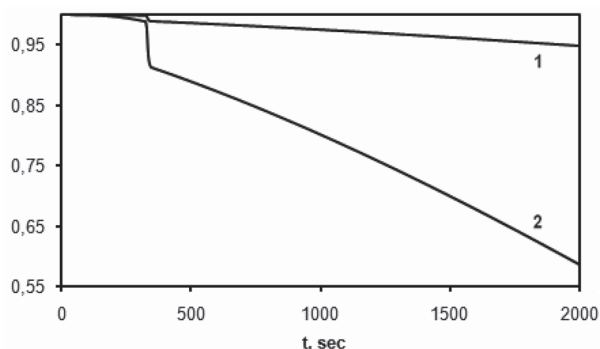

Fig. 3. Evolution of relative solute concentrations:
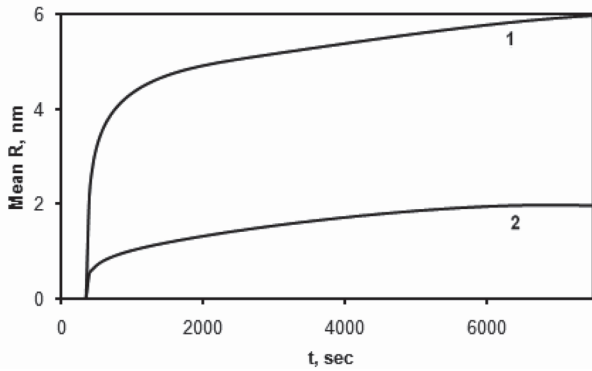*1* − c_{Mn} / c_{Mn_init} ; *2* − c_S / c_{S_init}

Fig. 4. Evolution of average radius of Cu$_2$S inclusions: *1* – particles with heterogeneous nucleation; *2* – homogeneous
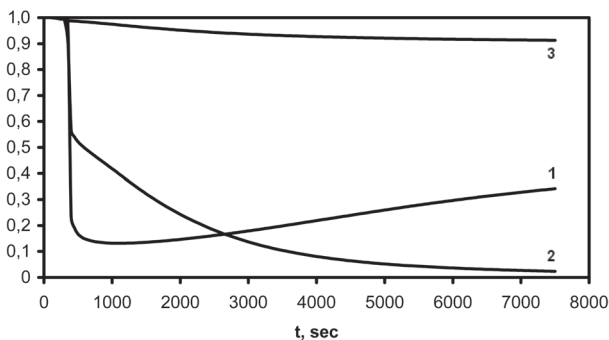

Fig. 5. Evolution of relative concentrations $c/c_{initial}$ in matrix: *1* – Cu; *2* – S; *3* – Mn

Simultaneous precipitation will be simulated in the following model: nucleation of MnS in γ-Fe; independent Cu$_2$S nucleation in α-Fe; simultaneous growth/shrinkage of precipitates.

In calculations it has been assumed in accordance with thermodynamical consideration [3], that atoms of Cu after shrinkage of Cu$_2$S inclusions transfer back to matrix for low Cu concentrations.

From the results of modeling after 2-hour annealing with independent nucleation of MnS and Cu$_2$S the following conclusions can be drawn:

1. Existence of both particles of Cu$_2$S with homogeneous nucleation (further homo-inclusions) and inclusions with heterogeneous nucleation (further hetero-inclusions).

2. The average radius of particles in homo-inclusions is about 1,5–2,0 nm and in hetero-inclusions 5–6 nm (Fig 4). The average radius of MnS inclusions is 60–70 nm.

3. Concentrations of Cu and S in matrix are quickly decreased at annealing onset. Further the sulfur concentration is decreased owing to MnS inclusions growth and Cu concentration is increased due to dissolution of copper sulfides inclusions, in the first place of homo-inclusions (Fig. 5).

4. The volume of homo-inclusions of copper sulfides is rapidly increased during initial stage of annealing (Fig. 6) with its subsequent decrease; the vol-

ume of hetero-inclusions is constantly increased with annealing time. After 2-hours annealing the volume of hetero-inclusions is ten times that of homo inclusions. The density of MnS inclusions during annealing is about 10^{18} nuclei·m^{-3}, the density of homo-inclusions is $1,3 \cdot 10^{24}$ nuclei·m^{-3} at annealing onset and $1,5 \cdot 10^{21}$ nuclei·m^{-3} after a two-hour interval; the density of hetero-inclusions is $8 \cdot 10^{20}$ nuclei·m^{-3} and approximately constant during annealing. Homo-inclusions «buffer» does not allow dissolving hetero-inclusions during the first 2 hours of annealing.

In reality sites for heterogeneous nucleation have different characteristics, and PSD for hetero inclusions can have greater width. For example, the region of density between the 2-nm average radius of homo-inclusions and 6-nm average radius of hetero inclusions can be well populated.

Of course, the model with continuous distribution of inclusion radius can not be used for proper prediction of kinetics behavior of Cu$_2$S particles when average size of particles is about a few atoms. But this model correctly predicts rapid nucleation and great density of inclusions. For quantitative prediction the fitting of initial density of possible sites and interface energy must be performed. With increasing the radius of inclusions the accuracy of CNGT model is increased.
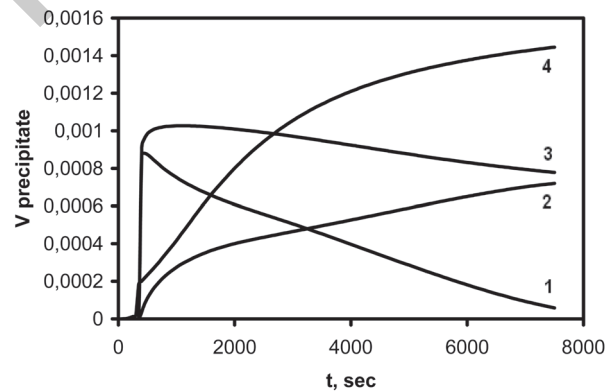

Fig. 6. Evolution of volumes of precipitates: *1* – copper sulfide homo inclusions; *2* – copper sulfide hetero inclusions; *3* – all copper sulfide; *4* – manganese sulfide
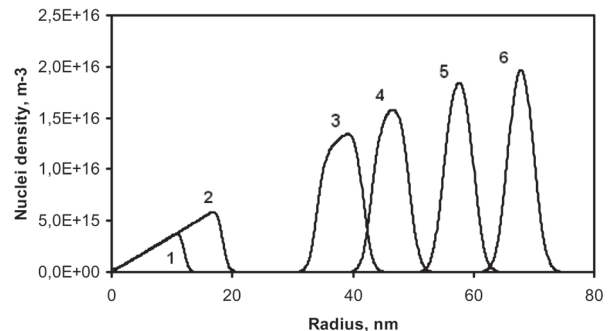

Fig. 7. PSD for MnS inclusions for different times: *1* – 100 sec after cooling beginning; *2* – 200; *3* – 500; *4* – 1000; *5* – 2000; *6* – 5000
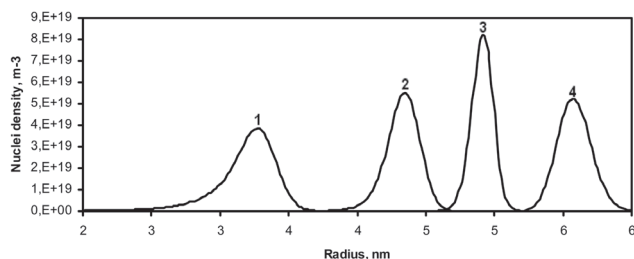
Fig. 8. PSD for hetero inclusions of copper sulfide: *1* – 500 s after process onset (about 200 sec after beginning of annealing); *2* – 1000; *3* – 2000; *4* – 5000
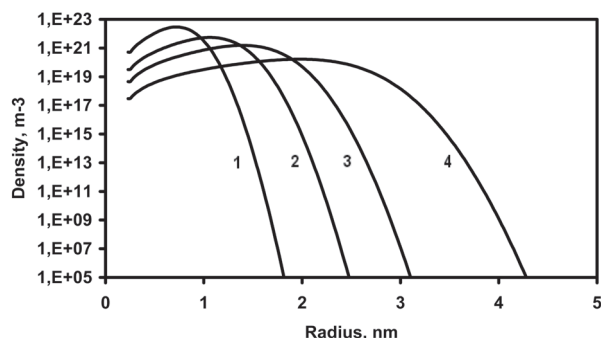

Fig. 9. PSD (logarithmic scale) for homo inclusions: *1* – 500 sec after beginning (about 200 sec after annealing start); *2* – 1000; *3* – 2000; *4* – 5000

Conclusions

Based on classical theory of nucleation and growth the precipitation of manganese and copper sulfides inclusions are modeled for solute concentrations of Cu equal to 0,07 wt%, S 0,04wt%, Mn 0,54wt % in iron matrix. The temperature regimes of steel working include cooling from 1200 °C to annealing temperature of 700 °C at cooling speed of 10 °C/sec and holding during 300 seconds at the temperature, that is slightly above that of γ-Fe – α-Fe transition used for MnS nucleation. It is assumed that the total possible heterogeneous nucleation density of modeling is 10^{20} nuclei/m^3 during such holding and 10^{21} at the annealing onset.

Inclusions of three types can be found in matrix such as copper sulfide formed by homogeneous nucleation mechanism with a size of about 4nm, copper sulfides formed by heterogeneous nucleation with size of 10–12 nm and manganese sulfide inclusions with size of 100–120 nm. Owing to different characteristics of heterogeneous sites the presence of Cu$_2$S inclusions

with intermediate size between 4 and 10 nm is also possible. Bimodal size distribution of overall copper sulfides precipitates is presented.

Densities of inclusions are highly dependent on initial solute concentration, temperature regimes of steel working and density of possible sites for heterogeneous nucleation. For manganese sulfide the heterogeneous nucleation is primarily responsible for inclusion formation due to high energy of matrix-precipitate interface. Nucleation occurs at the temperatures close to γ - α iron transition.

Copper sulfide inclusions are predominantly formed after annealing onset. Owing to small interface energy the high number of inclusions is formed following both homogeneous and heterogeneous schemes. Actually after a short period of ten seconds the cuprum solute concentration (or sulfur concentration if there is cuprum surplus for Cu$_2$S formation) is decreased in matrix due to a great number of possible sites for homogeneous nucleation.

Then inclusions grow during annealing. With heterogeneous nucleation copper sulfide inclusions reached 4-nm radius and 5-nm radius after 300-sec and 2000-sec annealing times, respectively; with homogeneous nucleation 1nm and 1.85 nm after 700 sec and approximately two hours, respectively. MnS inclusions have radius of 35 nm prior to annealing and 70 nm after 2-h annealing.

A great number of copper sulfide particles formed by homogeneous nucleation are sharply decreased. Sizable volume of such particles is also quickly decreased. But such «buffer» enables growing the inclusions formed by heterogeneous nucleation due to a greater size of the latter. The volume of inclusions, created by heterogeneous mechanism is also increased during 2-h annealing.

Some general results obtained for densities can be also presented. So, manganese sulfide density is about 10^{-2}–10^{-3} relative overall density of heterogeneous sites. Density of copper sulfides inclusions created by homogeneous scheme is 10^{22}–10^{24} nuclei·m^{-3} before annealing and 10^{20}–10^{21} after two-h annealing. Density of inclusions obtained by heterogeneous scheme is about total number of possible heterogeneous sites.

References

1. H o n g M. H., C h o i K. Y., M a r u k o v i c h E. I., L e b e d i n s k y Y. A., B r a n o v i t s k y A. M. Modeling of precipitation kinetics of manganese and copper sulfides in interstitial free steels // Литье и металлургия. 2009. № 4. С. 39–43.

2. L i u Z., K o b a y a s h i Y., N a g a i K. / Crystallography and Precipitation Kinetics of Copper Sulfide in Strip Casting Low Carbon Steel // ISIJ Int. 2004. Vol. 44. P. 1560–1567.

3. L e e B.- J., S u n d m a n B., I l K i m S., C h i n K.- G. Thermodynamic Calculations on the Stability of Cu$_2$S in Low Carbon Steels // ISIJ Int. 2007. Vol. 47. P. 163–171.